ROYAL SOCIETY OF CHEMISTRY

PAPER

Check for updates

Colloidal silica nanomaterials reduce the toxicity of pesticides to algae, depending on charge and surface area†

Frida Book, [iD] *[a] Michael Persson,[b] Eric Carmona,[c]
Thomas Backhaus[a] and Tobias Lammel [iD] [a]

Colloidal silica nanomaterials are promising adsorbents for aquatic pollutants. The present study quantifies the toxicity reduction of differently charged pesticides (paraquat (cationic), pentachlorophenol (anionic) and diflufenican (uncharged)) by co-exposure to weakly anionic, strongly anionic and cationic silica nanomaterials in growth tests with freshwater green algae. The hypothesis was that the silica nanomaterials would preferentially adsorb the oppositely charged pesticide and reduce algal toxicity accordingly. Three different concentrations of each spherical nanomaterial (10, 20 and 50 mg L^{-1}) were tested in mixtures with a fixed pesticide concentration (4 μM paraquat (EC60), 0.002 μM diflufenican (EC80) and 0.2 μM penta-chlorophenol (EC90)). In addition, we investigated the role of the specific surface area by comparing the performance of the anionic spherical silica nanomaterial with the anionic elongated silica nanomaterial (0.4–16 mg L^{-1}). Adsorption of pesticides onto the various nanomaterials was confirmed by chemical analysis of the supernatants after removing the nanomaterial with ultracentrifugation. The results show that a concentration of 16 mg L^{-1} and 50 mg L^{-1} of the spherical and elongated strongly anionic silica, respectively, completely annulled paraquat toxicity. The cationic nanomaterial reduced pentachlorophenol toxicity by 30–50% at all test concentrations, but the effect seems to be influenced by pH and phosphate concentration of the test medium. The cationic silica also reduced the toxicity of diflufenican by 10–20%, likely due to non-electrostatic interactions. The study further indicates that the presence of algae affects the NM–pesticide equilibrium since the pesticide is taken up by the organism instead of being bound to the NM.

Environmental significance

Silica NMs show promising properties as adsorbents for aquatic contaminants through electrostatic interaction. The current evidence for using them in this context is however limited and even less is known regarding the NM's adsorption efficiency in the presence of aquatic organisms that are most likely to co-occur and therefore be subject to toxic exposure and affect the nanomaterial-chemical interplay. Here, we investigate the toxicity of charged pesticides to freshwater green algae in the presence of oppositely charged silica NMs. Our results show that strongly charged colloidal silicas are efficient adsorbents of oppositely charged pesticides, which leads to a significant reduction in toxicity towards algal cells and that the presence of algal cells likely reduces the adsorption capacity of the NM.

1. Introduction

Manufactured nanomaterials (NM) are efficient adsorbents because of their large specific surface area[1] and high surface energy.[2] Adsorption of chemicals to the NM surface lowers the surface energy, helping to reach an energetically preferable state.[2,3] The intermolecular forces attracting the adsorbate onto the adsorbent may include van der Waals, hydrogen bonding, electrostatic interaction, covalent bonding and hydrophobic forces.[4–6]

These properties can be beneficial for different technological applications. For example, NMs can potentially remove a wide range of potentially hazardous chemicals from water including pharmaceuticals, pesticides, heavy metals, chlorinated solvents, dyes and per- and polyfluoroalkyl substances (PFAS).[7–9] They can also be used to carry pesticides and release them in a controlled way, reducing the total amount of pesticide that needs to be applied and thereby reduce adverse impacts on non-target organisms.[10,11]

[a] *Department of Biological and Environmental Sciences, University of Gothenburg, Gothenburg, Sweden. E-mail: frida.book@gu.se*
[b] *Chalmers Industriteknik (CIT), Gothenburg, Sweden*
[c] *Helmholtz Centre for Environmental Research (UFZ), Leipzig, Germany*

The wide and large use of pesticides is currently causing a significant risk to the aquatic environments (both autotrophs and heterotrophs species)[12–14] and measures for reducing their concentrations in waters are therefore coveted.[15,16] Silica NMs (or nanocomposites containing silica) are particularly suitable for use in applications mentioned above because of their facile preparation and a number of unique properties, including thermal stability, mechanical strength, tunable structure (shape and porosity), biocompatibility and a surface allowing functional modifications.[17–19] Various studies have demonstrated that silica NMs can be used to bind and remove both organic and inorganic chemicals with potentially harmful properties (pesticides and heavy metals) from water, and that adsorption efficiency was dependant on NMs surface chemistry.[10,17,20] Silica NMs can also be engineered to have an iron core which allows to remove adsorbed pollutants from the water phase by applying a magnetic field while the silica shell prevents the iron from oxidation, gives chemical stability and enables customized surface functionalization.[21]

A subgroup of silica nanoparticles is colloidal silica, consisting of suspended amorphous spherical particles (5–100 nm).[22] Commercial products of colloidal silica can have various electrostatic properties, which is typically achieved *via* surface modification with aluminium species resulting in increased anionic or cationic charge depending on how the aluminium is incorporated on the surface.[23,25] These products have been shown to remain stably suspended when diluted in aqueous media with a broad range of ionic strengths.[24] For water treatment, this could be an advantage since it increases the residence time for which the NM can bind the pollutant, in comparison with other in general more hydrophobic NMs, such as carbon-based NMs, which are more prone to agglomerate and settle out.[1,20,26] Colloidal silica is used as a flocculation agent and binder in the paper and ceramic industry,[27,28] but its properties as an adsorbent in the context of water purification is less well described.[1,20,26]

Published studies typically use laboratory systems that comprise merely the NM and a pollutant, but no aquatic organisms, which could be subjected to toxic exposure[1,20,26] or compete/interfere with the NMs' capacity to adsorb the pollutant.[29] For example, nanoparticles may modify the uptake of environmental co-existing contaminants and *vice versa* leading to an increase or decrease in toxicity compared to the toxicity caused by the compounds alone.[30] To the best of our knowledge, few mixture exposures of silica NMs and other contaminants to aquatic organisms have been published yet.[31] Martín-de-Lucía *et al.*[32] exposed the bioluminescent cyanobacterium *Anabaena* sp. to silica NMs and wastewater, which resulted in a decreased toxicity attributed to the adsorption of wastewater pollutants onto the silica surface. Cui *et al.*[33,34] also report a reduced toxicity of Cd and As to rice cells in the presence of silica NM likely due to adsorption of Cd and As onto the silica.

The objective of the present study was to investigate the toxicity of herbicides to the freshwater green algae *Raphidocelis subcapitata* (formerly known as *Pseudokirchneriella subcapitata*) in the presence of colloidal silica NMs with different charge (surface functionalization) and shape (spherical and elongated NMs). We hypothesized that charged particles predominantly bind oppositely charged herbicides, thereby reducing bioavailability and algal toxicity. To test this hypothesis, strongly charged NMs (cationic and anionic) as well as one weakly anionic NM (non-modified bare silica) were mixed together with the herbicides paraquat (cationic), pentachlorophenol (anionic) or diflufenican (neutral) in separate algal growth experiments. We also tested whether elongated strongly anionic NM, with a larger specific surface area, adsorb a larger amount of the herbicide in comparison to the spherical strongly anionic NM. The three herbicides paraquat, pentachlorophenol and diflufenican were chosen as model compounds with different charges, because of their well known toxicity to *R. subcapitata*[35–37] their chemical stability under the conditions of the test and the availability of well-established analytical methods. In addition, diflufenican belongs to the group of fluorinated pesticides with a significant market share in the agricultural sector, and is one of the herbicides with the highest exceedance rate of the environmental quality standards in European surface waters.[38,39]

2. Materials and method

2.1 Nanomaterials

All tested NMs are listed together with their main characteristics in Table 1. They were obtained as aqueous suspensions from Nouryon (Sweden) and belong to the Levasil® colloidal silica product line. These and similar NMs are widely used as binders and flocculation agents in the pulp and paper industry in order to bind oppositely charged debris. The test material comprised of four different NMs: three spherical particles, having different charges (weakly anionic, strongly anionic and cationic) and a fourth elongated NM, also with a strongly anionic spherical NM. The anionic and cationic NMs are surface modified with aluminium species, either attached onto the surface (cationic, *i.e.*, aluminium chlorohydrate) or incorporated into the surface (strongly anionic, *i.e.* sodium aluminate), Fig. 1. The weakly anionic NM is not surface-modified and the surface charge results from deprotonated silanol groups.

The silica NMs supplied by the manufacturer have different surface areas, 160 m^2 g^{-1} (cationic), 360 m^2 g^{-1} (weakly anionic and strongly anionic) and 1100 m^2 g^{-1} (strongly anionic elongated). The NMs were sampled directly in the production line before chemical preservatives (biocides) are added, which would cause toxic effects on the NM-exposed algae that would interfere with the measurement of NM toxicity. Information reported in Table 1 and Fig. 1 were obtained from the manufacturer. Electron microscopy images of the cationic and the elongated NM are presented in Fig. S5 and S6.† Electron microscopic photos of the other NMs are presented in our previous study.[24]

This journal is © The Royal Society of Chemistry 2022

Environ. Sci.: Nano, 2022, **9**, 2402–2416 | **2403**

Table 1 List of the stock colloidal silica nanomaterials used in the study with information provided by the supplier. The nanomaterials are presented with product name, shape, mean average size, measured specific surface area (SSA), silica content, pH, surface chemistry, charge and relative charge density

Product name	Shape	Average particle size[a] (nm)	Measured SSA[b] ($m^2\ g^{-1}$)	Silica (wt%)	pH	Surface chemistry	Charge
Levasil® CS30-236	Spherical	17	360	30	8–11	Non-modified	Weakly anionic
Levasil® CS25-436	Spherical	20	360[c]	25	5–11	Aluminium-modified	Strongly anionic
Levasil® RD 2180	Elongated	5 (particles attached in a chain)	1100[c]	6.5	5–11	Aluminium-modified	Strongly anionic
Levasil® CS30-516P	Spherical	35	160[c]	25	2–5	Aluminium-modified	Cationic

[a] Number average measured with electrospray differential mobility analyser (ES-DMA).[40] [b] SSA measured by Sears titration.[41] [c] SSA before surface modification with aluminium.

2.2 Pesticides

Paraquat (PQ) (CAS nr 75365-73-0) and diflufenican (DFF) (CAS nr 83164-33-4), were purchased from Sigma-Aldrich (Merck KGaA). pentachlorophenol (PCP) (CAS nr 87-86-5), was supplied by Supelco® Analytical (Merck KGaA). The pesticides have different modes of action and charges: PQ blocks the electron transport chain at photosystem I and carries a (pH-independant) positive net charge due to two quaternary nitrogen atoms (Table 2), DFF is an uncharged molecule that inhibits carotenoid biosynthesis, and PCP exerts its pesticidal action as an uncoupler of oxidative phosphorylation and carries a negative charge at neutral pH.

2.3 Nanomaterial characterization

Hydrodynamic size distribution and charge were measured by dynamic light scattering (DLS) analysis using disposable polystyrene macro cuvettes (VWR International AB, Gothenburg, Sweden) and a Malvern Zetasizer Nano ZS (Malvern Instruments Ltd., Malvern, UK). Initially, size and charge were measured for NMs diluted in Milli-Q water at a concentration of 5000 mg L^{-1}, in order to resemble the characteristics in the initial stock suspensions obtained from the manufacturer. Consequently, the NMs were characterized in the exposure medium (ionic strength 2.23 mM and pH 7.2 ± 0.5), with and without the presence of the pesticide and at the maximum and minimum NMs concentrations used in both single and mixture exposures, 10, 20, 50, 150 and 500 mg L^{-1} for the spherical NMs and 0.4 mg L^{-1}, 10 mg L^{-1}, 20 mg L^{-1}, 50 mg L^{-1} and 150 mg L^{-1} for the elongated NM.

Fig. 1 Surface chemistry of the three different nanomaterials used in the study. Non-modified with a weakly anionic charge (to the left), aluminium-modified with a strong anionic charge (middle) and aluminium-modified with a cationic charge (right). Information on the surface chemistries was retrieved from the Nouryon web page and correspond to the original stock product.[25]

These measurements were conducted immediately after preparing the mixtures (t_0) and at the end of the test duration (72 h).

For size measurements, four consecutive measurements at ten runs were conducted at 22 °C using a 173° backscatter detection. The attenuation level and optimum measurement position was automatically set by the instrument. Zetapotential (ZP) measurements were conducted after 120 seconds of calibration time and with three consecutive measurements at 22 °C per sample. Number of required runs per measurement, measurement position, attenuator level and voltage was automatically set by the instrument. The Smoluchowski approximation was set as default, but an approximation of Henry's function for particles with a radius around or below 12.5 nm in accordance with Duan et al.[42]

2.4 Algae toxicity assay

In the first set of experiments, the algae were exposed to NMs and pesticides separately, in order to establish the individual concentration–response curves as the basis for selecting the concentration range for the mixture experiments. The experiments (both individual and mixtures exposures) were conducted with the green freshwater algae species *R. subcapitata* (strain 61.81 from Experimental Phycology and Culture Collection of Algae (EPSAG), Göttingen, Germany). The assay was performed following the organisation for Economic Co-operation and Development (OECD) guidelines (test no. 201) with a start cell density around 15–20 000 cells per mL, but using 96-well plates, a 16 : 8 h light : dark cycle and MBL exposure medium.[45] The light and temperature were kept stable at 100 ± 5 μEm^{-2} s^{-1} and 22 °C ± 2 °C. As a proxy for growth, chlorophyll fluorescence was measured both at t_0 and after 72 h by measuring the 96-well plates in a fluorometer (Varioskan Flash version 4.00.53) at the excitation/emission wavelengths 425 nm/680 nm. The exposure time (t_0 – 72 h) was sufficient to obtain a ≥16-fold growth of the unexposed algae, a requirement of the OECD guideline. Growth inhibition was expressed in percentage and calculated by subtracting the fluorescence of the blank (medium only) from the sample fluorescence and then normalizing to the fluorescence of unexposed algae. All outer wells of the microtiter plate were used as blanks only, as
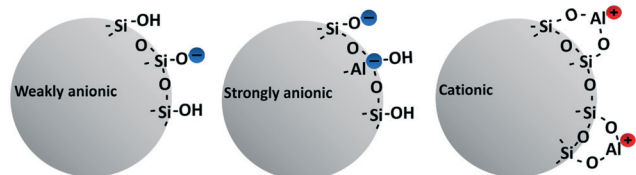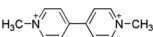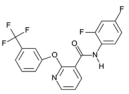
Table 2 List of pesticides used in the study. The pesticides are presented with name, CAS Nr, structure, pK_a, net charge at pH 7, $\log P$ and mode of action. Charge at pH 7 was determined based on the chemical structure of the pesticide or the pK_a

Pesticide	CAS nr	Structure[a]	pK_a[b]	Net charge at pH 7	Log P[b]	Mode of action[b]
Paraquat	4685-14-7		Not applicable	+2	−4.5	Photosystem I (electron transport) inhibitor
pentachlorophenol	87-86-5		4.7 (weak acid)	−1	3.3	Uncoupler of oxidative phosphorylation
Diflufenican	83164-33-4		Not applicable	0	4.2	Inhibition of carotenoid biosynthesis (bleaching)

[a] Chemical structures were retrieved from Wikimedia commons website.[43] [b] pK_a, $\log P$ and mode of action were retrieved from the Pesticide Properties DataBase (PPDP).[44]
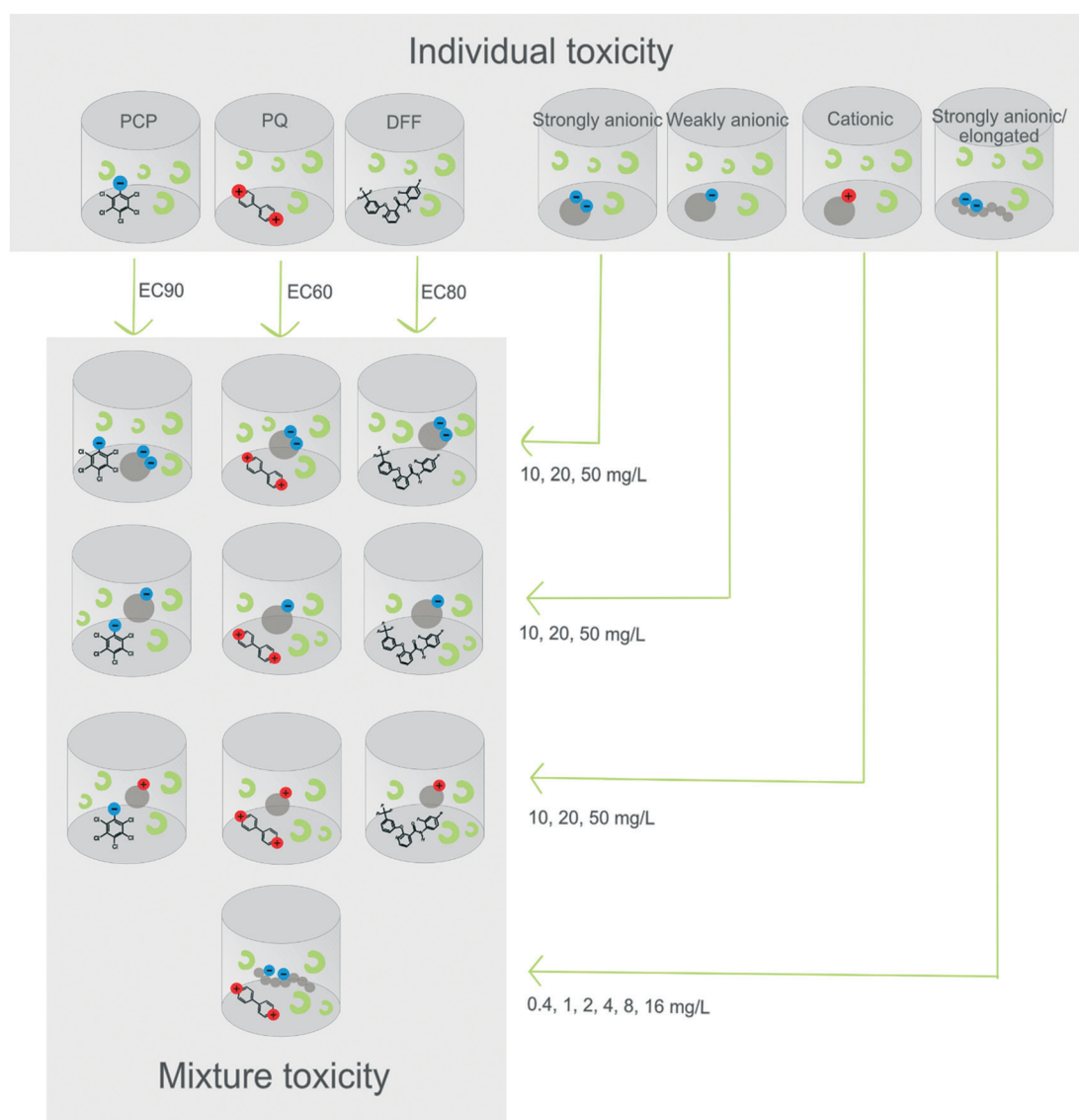

Fig. 2 Illustration of the experimental workflow. In a first set of experiments, the algae were exposed to the pesticides and the NMs separately. In a second step of experiments, PCP (EC90), PQ (EC60) and DFF(EC80) were tested in mixture with the spherical silica NMs (weakly anionic, strongly anionic and cationic) at the concentrations 10, 20 and 50 mg L^{-1} or elongated strongly anionic NM (0.4–16 mg L^{-1}). Effects measured for mixtures were compared with those in single substance controls (not shown).

This journal is © The Royal Society of Chemistry 2022

Environ. Sci.: Nano, 2022, **9**, 2402–2416 | **2405**

outer wells are exposed to an increased air-exchange and have a higher evaporation rate. At least 3 technical replicates were measured per plate and 30 unexposed controls were used per plate.

After establishing the individual concentration–response curves of the different NMs and the pesticides, the algae were exposed to three NM concentrations (10, 20 and 50 mg L^{-1}) in mixtures with one fixed concentration of the pesticide, known to cause a >50% effect: 4 μM (1029 μg L^{-1}) PQ (EC60), 0.002 μM (0.8 μg L^{-1}) DFF (EC80) and 0.2 μM (53 μg L^{-1}) PCP (EC90) (Fig. 2). In addition, only NM controls (0.4, 10, 16, 20 and 50 mg L^{-1}), only pesticide control (4 μM PQ, 0.002 μM DFF or 0.2 μM PCP), negative controls (unexposed algae) and medium control (blank) were included in each 96-well plate to account for inter-plate and inter-experiment variation. The elongated NM was only tested in a binary mixture experiment with PQ, in order to compare it to the growth inhibition after exposure to the mixture of PQ and spherical NM with the similar strong anionic surface charge. Furthermore, because of its comparatively higher specific area (1100 m^2 g^{-1}) it was tested at lower mass concentrations (0.4–16 mg L^{-1}) so that they had similar exposure surface areas.

2.4.1 Preparation of test suspensions from stocks to 96-well plates

2.4.1.1 Individual concentration–response curves for the different nanomaterials. The stock suspensions (supplied by the company) were diluted in two steps, first in Milli-Q water to a concentration 133 times stronger than the highest test concentration and then diluted 1:100 in medium. A volume of 150 μL of this highest test concentration was then added to each of the three wells B3–C3 followed by a two-fold dilution series performed directly in the plate (for a detailed view of the plate design see the ESI† Fig. S1). Thereafter, 50 μL of algae suspensions was added/well resulting in NM concentrations of 1–500 mg L^{-1} for the spherical NMs and 0.3–150 mg L^{-1} for the elongated NM in a total volume of 200 μL per well.

2.4.1.2 Exposure to nanomaterial–pesticide mixtures. Mixing PQ and DFF with NMs was done directly in the 96-well plate. The NM stock suspensions (supplied by the company) were diluted in two steps, first in Milli-Q water to a concentration 233 times stronger than the highest test concentration and then 1:100 in medium. Consequently, a volume of 100 μL of the prepared particle suspension in medium was added to the plate followed by 50 μL of pesticide (4 times the final test concentration in medium) and lastly 50 μL algae suspension, to a final volume of 200 μL per well.

Mixtures comprising PCP and cationic NM were prepared according to two different protocols in order to investigate if negatively charged phosphate ions naturally present in the medium, and known to bind to cationic colloidal silica nanoparticles,[23] compete with PCP for binding to the NMs surface. The first protocol corresponded to the one used for the preparation for the mixtures with PQ described above, that is, the NM and pesticide were mixed in the well plate. The second protocol consisted in mixing the NM and pesticide in a separate vial, that is, prior to their addition to the well plate. This premix, which had a 133 times stronger concentration than the test concentration desired in the assay, was incubated for 4 h ± 1 h at room temperature. Subsequently, it was diluted 1:100 in medium and 150 μl aliquots were added to the wells of the plate. The pre-mixing step was included to increase the chance for the PCP to adsorb onto the cationic NM by electrostatic interaction due to a lower phosphate ion to NM concentration ratio. To enable comparison, the PCP mixtures with the other two NMs, that is, the anionic and non-modified NMs, were also prepared in this way (through preparation of a 133 times stronger pre-mixture).

A detailed view of the plate design for the mixture exposures is presented in Fig. S2.†

2.5 Interference control

To investigate if the NMs interfere with fluorescence readout at the excitation and emission wavelengths used in the algae toxicity assay, absorbance at 425 nm and 680 nm was measured at seven concentrations between 1–64 mg L^{-1} using a Varioskan Flash (version 4.00.53) photometer. Absorbed light in percentage was calculated from non-transmitted light in accordance to a previous study.[24]

2.6 Modelling of concentration–response curves

Modelling of concentration–response curves and effects concentrations exerting *x*% effect (EC*x*) values was conducted in R (version 3.6.3) by comparing the best fit of three different two-parameter models: weibull, logit and probit. The best fit was determined based on visual inspection and by comparing lowest residual standard errors. The equations used are the following:

$$\text{Weibull: } 1 - \exp(-\exp(\theta_1 + \theta_2 \times \log 10(\text{conc})))$$

$$\text{Logit: } 1/(1 + \exp(-\theta_1 - \theta_2 \times \log 10(\text{conc})))$$

$$\text{Probit: } \text{pnorm}(\theta_1 + \theta_2 \times (\log 10(\text{conc})))$$

where parameters θ_1 describes the location and θ_2 the steepness of the curve.

2.7 Scanning electron microscopy

Algae exposed to 50 mg L^{-1} of NM for 72 h were imaged by scanning electron microscopy (SEM). After the 72 h exposure, 1 mL of each sample was loaded onto a silica wafer 0.25 mm^2 pre-coated with poly-L-lysine placed into a well of a 4-well plate. The samples were fixed in 0.1 M Karnovsky's fixative in cacodylate buffer and subsequently in osmium tetroxide (1% in water). The immersion in Karnovsky's fixative lasted for 30 min followed by three washes with glycine in cacodylate buffer and two times with water.

2406 | *Environ. Sci.: Nano*, 2022, **9**, 2402–2416

This journal is © The Royal Society of Chemistry 2022

Osmium tetroxide was added to the samples 3 times 5 min at room temperature. Consequently, the samples were dehydrated in an ethanol series (30, 50, 70, 85, 95 and 3 times 100% with 5 min at each step). The samples were then incubated with hexamethyldisilazane for two minutes and then left to evaporate. Prior to imaging, the samples were mounted on a 11 mm aluminium stub with a 12 mm carbon tab and then imaged with a ZEISS Gemini(2)SEM 450 with a Denka Thermal FEG gun.

2.8 Pesticide adsorption onto the nanomaterials

The particles ability to adsorb the various pesticides was investigated through chemical analysis after the NMs had been removed by ultracentrifugation. NM suspensions with concentrations corresponding to the lowest and highest used in the exposures were prepared as described in section 2.4.1.2, but without algae. The samples were ultracentrifuged (Beckman Coulter Allegra X-15R) at 312 000 g for 2 h in 4 ml open-top thickwall polycarbonate tubes. These conditions were chosen because they were sufficient for removing NM in previous studies,[46] which was also verified in the present study by running DLS analysis on the supernatants. Directly after ultracentrifugation, 1 ml of the supernatant was taken out and added to 1.5 mL brown glass vials and stored at −18 °C. All ultracentrifugation samples were run in triplicates and included three different controls consisting of only medium, only NM and only pesticide. The recovery of the pesticides (*i.e.*, the amount of pesticide in the supernatant following ultracentrifugation in relation to the amount of pesticide initially added/before ultracentrifugation) was determined by including a pesticide-recovery control. The total pesticide content in each sample was analysed using LC-MS.

2.8.1 Chemical analysis.
For the analysis of DFF and PCP, 25 μL of the samples were injected into an Agilent 1260 HPLC system, in tandem with a Qtrap 6500 from ABSciex. The chromatographic separation was performed on a Kinetex C18 column with a gradient of water with 0.1% formic acid (A) and 0.1% formic acid in methanol (B), starting with 300 μL min^{-1} as a flow rate and 40% of phase B. For the analysis of PQ, 10 μL of each sample was injected. For separation, an Acclaim Trinity Q1 100 × 3 mm column was used, and a gradient of 100 mM NH$_4$–acetate in water (A) and acetonitrile (B) was employed. The gradient started with 35% of acetonitrile. The MS1 was set to full scan mode. The column temperature was 40 °C. DFF was measured in positive mode with the precursor ion 395 and the product ions 266, 246 and 218. PQ was measured in positive mode with the precursor ion 185 and the product ions 170, 169 and 144. PCP was measured in negative mode with the ions 263, 265 and 267 (the fragmented part chlorine was not used, since this would offer a poor second ion). The chromatograms were processed with the Sciex MultiQuant 3.0 software with a calibration line between 0.01 ng mL^{-1} until 2000 ng mL^{-1}, fitting to a regression line with an $R^2 > 0.97$.

3. Results and discussion

Here we explore if silica NMs with specifically engineered surface chemistries can be used to efficiently and selectively remove potentially hazardous contaminants from aqueous solutions. The hypothesis of the study was that charged silica NMs would attract oppositely charged pesticides reducing their availability and consequently algal toxicity. A second hypothesis was that the elongated NM would be superior to spherical NMs in adsorbing the pesticide due to a larger specific surface area. Prior to choosing the concentration for mixture exposures, individual toxicity of NMs and pesticides were determined.

3.1 Individual toxicity

3.1.1 Toxicity of silica nanomaterials.
The experiments clearly show that silica NMs with different surface chemistry and charge have different algal toxicities. While Levasil CS25-436 and Levasil RD 2180 are non-toxic up to concentrations of 500 mg L^{-1} and 150 mg L^{-1}, respectively, both Levasil CS30-236 and Levasil CS30-516P show a distinct concentration–response relationship (Fig. 3). SEM analysis of exposed algae indicate that the difference in toxicity might be due to differential interaction with the cell walls (Fig. 4) in increasing order, strongly anionic < weakly anionic < cationic. The weakly anionic and cationic NMs adsorb well to the algae surface, and the cationic NM also flocculates the algae cells. It is likely that NM adsorption reduces the amount of light that reaches the cell, thereby reducing growth, which is in accordance with the "shading effect" proposed in earlier studies.[23,47–49]

Van Hoecke *et al.*[23] suggested that the flocculation is driven by the electrostatic interaction between the positively charged NM and the negatively charged algal cells. However, as mentioned before and according to the ZP measurements in the present study, this NM seems to no longer carry a distinct positive charge when they are exposed to the algae, which would question this theory. Instead, this might be owed to the low colloidal stability of the catsol (cationic colloidal silica), which could result in NMs aggregating on algae and flocculating them. In addition, phosphate (adsorbed onto the cationic NM) could act as a glue bringing algae and the NM together, since phosphate uptake by algae is suggested to be a two-stage process comprised of adsorption of phosphate onto the algae surface before internal uptake.[50,51] However, the full explanation for what is driving this cell–particle–cell interaction needs to be addressed by future research.

3.1.2 Pesticide toxicity.
Exposure to the different pesticides results in a clear concentration–response relationship (Fig. S3†) in the tested concentration range (0.1–195 μM (PQ), 0.03–0.45 μM (PCP) and 0.0002–0.015 μM (DFF)), with EC50 values of 3.1 μM for PQ, 0.12 for PCP μM and 0.0013 μM for DFF, respectively. The fixed pesticide concentration for the mixture exposures was based on the requirements that it should have a high effect level, in order to be able to observe
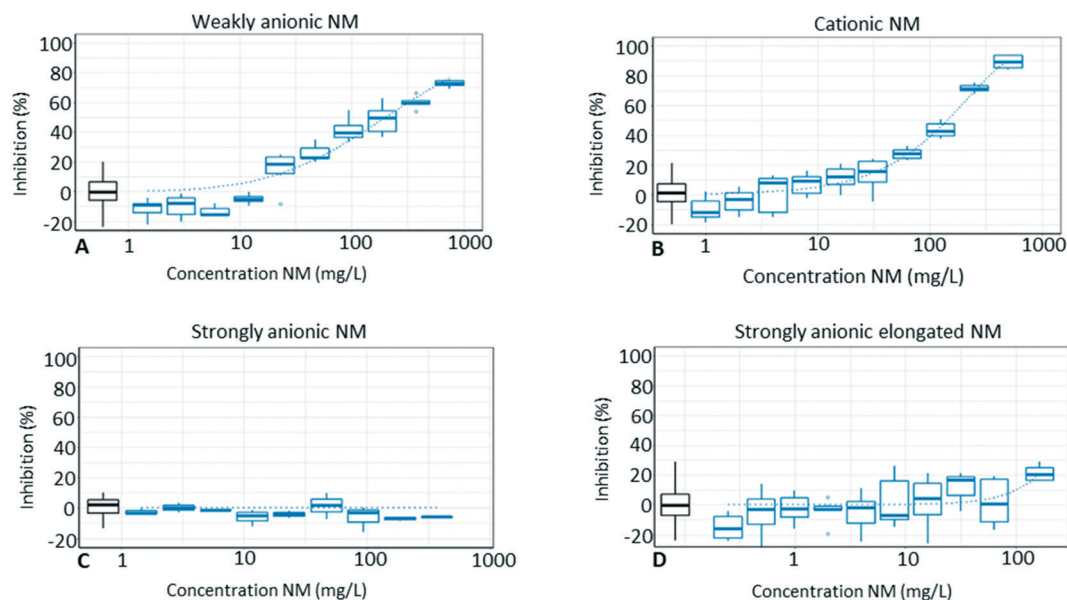
This journal is © The Royal Society of Chemistry 2022

Environ. Sci.: Nano, 2022, **9**, 2402–2416 | **2407**

Fig. 3 Concentration–response relationships for the different silica nanomaterials (NMs), weakly anionic (A), cationic (B), strongly anionic (C) and strongly anionic elongated (D). The boxes show the inhibition (median, lower/upper quartile, and lower/upper extreme) at the tested concentration and the dotted line shows the fitted curve calculated from a two-parametric concentration–response model. The box shown in black colour (first box from left) represents the unexposed control.

a reduction in toxicity. Therefore, we chose concentrations above the EC50 value and below the upper asymptote. The

Fig. 4 SEM images showing charge-dependant adsorption of NMs onto the algae the cell wall after 72 h exposure to 50 mg L^{-1}. Image A shows the unexposed algae (control) at a magnification of 26 000×, B depicts cells exposed to the strongly anionic NM (magnification 35 000×), C shows algae exposed to the strongly anionic elongated NM (magnification 35 000×), D shows algae exposed to the weakly anionic NM (magnification 26 000×) and E and F depicts algae exposed to the cationic NM after imaging with SEM (E) (magnification of 7000×) or a light microscope (F) (magnification of 40×).

resulting fixed effect concentrations of the pesticides used for mixture experiments in the end were 4 μM for PQ (EC60), 0.2 μM for PCP (EC90) and 0.002 μM (DFF). The chosen exerting effect of PQ was slightly lower than for PCP and DFF, in order to not use an excessively high concentration of PQ and thereby avoiding an overload of the adsorption capacity of the NM. However, the effect concentration for PCP did not strictly meet the initial requirement since the effect varied with up to 30% between experiments (Fig. 6). One hypothesis for this larger variation could be the PCP's comparatively narrow concentration window where its exerted toxicity was extra sensitive to inter-experiment variations.

3.2 Mixture exposures with PQ

The results from the mixture exposures show that strongly anionic silica NMs reduce the toxicity of PQ, whereas 50 mg L^{-1} of the spherical and 8–16 mg L^{-1} of the elongated strongly anionic NM annul the toxicity of PQ completely (no difference in comparison to the unexposed control, Fig. 5C and D). In contrast, Levasil CS30-236 (weakly anionic) and Levasil CS30-516P (cationic) do not reduce the toxicity of PQ. This is in agreement with our hypothesis that PQ adsorption depends on both NM surface charge and surface area. The adsorption of PQ onto the NMs is confirmed by the chemical analysis of the supernatants during which almost no free PQ was detected in the growth medium after NM co-exposure (Table 4). This observation corresponds to previous results by Brigante and Schulz[52] who also observed an increased adsorption capacity for surface-modified silica with increasing anionic charge. Furthermore, while the chemical analysis shows that all NMs are able to adsorb PQ, there was
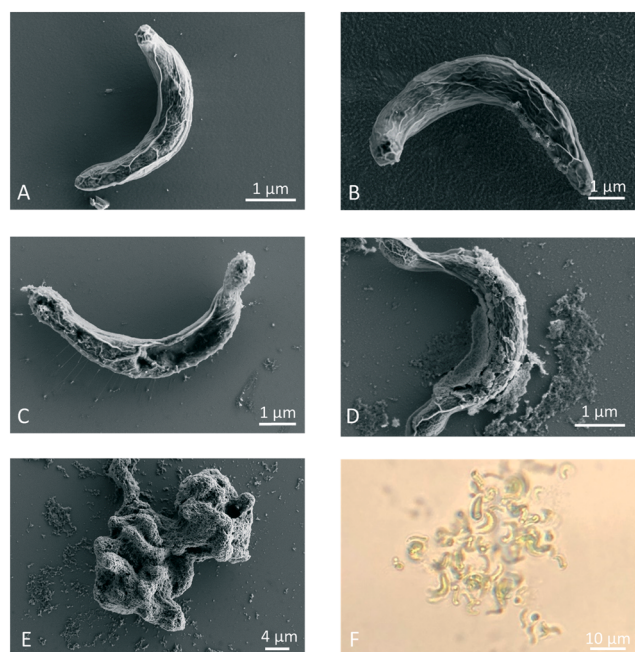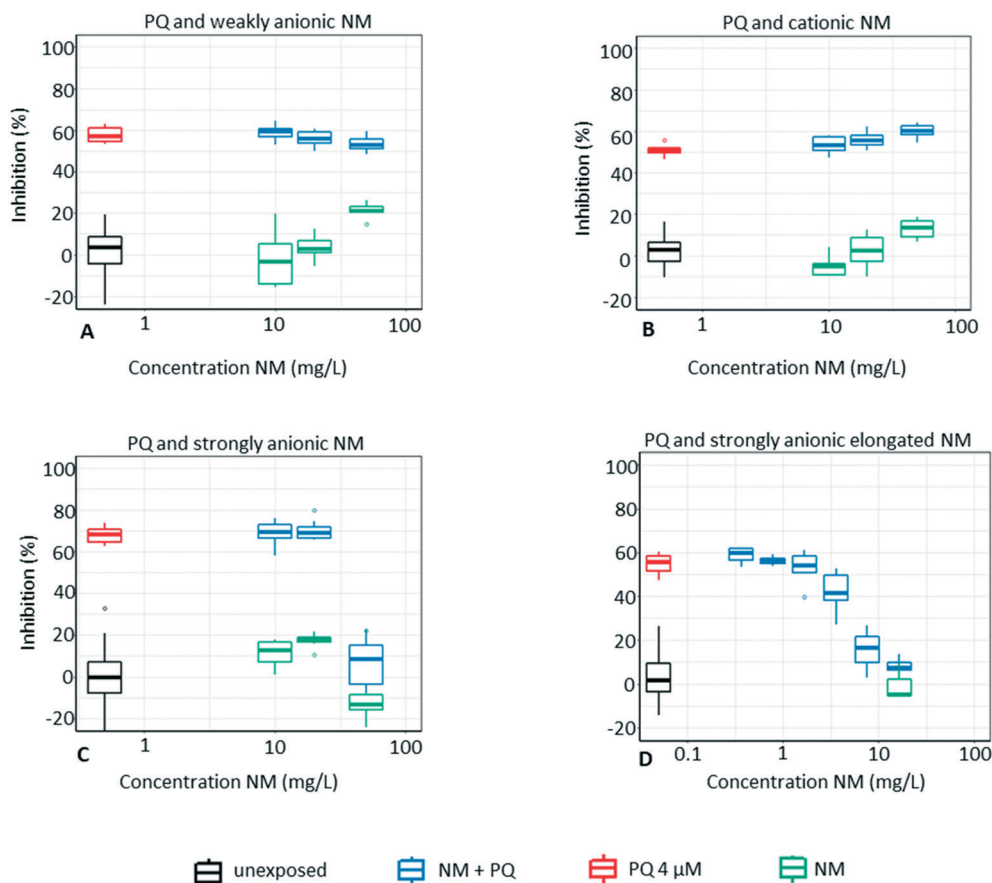
Fig. 5 Effects of binary mixtures of PQ and silica NM with different surface chemistry on algae growth. The mixtures comprised of PQ (4 μM) in binary mixture with the weakly anionic NM (A), cationic NM (B), strongly anionic NM (C) and strongly anionic elongated NM (D) at 10, 20 and 50 mg L^{-1} (blue boxes). The black boxes represent the unexposed algae (control), the red box shows results from exposure to only PQ and the green boxes represent the inhibition after exposure to only the NM. The boxplots show the median, quartile 1 (Q1), quartile 3 (Q3) and the maximum (Q3 plus 1.5 times the interquartile range) and minimum (Q1 minus 1.5 times the interquartile range).

a clear trend in the amount of PQ adsorbed to the different NMs (strongly anionic > cationic > weakly anionic).

Surprisingly, the cationic spherical NM adsorbs significant amounts of PQ, and already the lowest test concentration of 10 mg L^{-1} NM reduces the PQ content by 60%. This decrease in PQ bioavailability should translate into a reduced algal toxicity, which however is not observed (Fig. 5B). An explanation for this could be that the uptake of freely available PQ molecules by algae shifts the chemical equilibrium driving PQ to desorb from the NM. From an electrostatic perspective, the cationic NM's ability to adsorb PQ seemed less likely in advance. However, the ZP measurements reveal that the charge of cationic NM changes becoming slightly negative in the exposure medium (see Table S1†), which could be due to the adsorption of anions (such as phosphate) onto the surface in combination with a precipitation of the surface aluminium (Al^{3+}) to aluminium hydroxide (Al(OH)$_3$) which is expected to occur with time at pH >5 (Michael Persson, personal communication, November 2, 2021). This slightly negative charge at the surface of the cationic NM could be enough to attract PQ. Another possibility could be that PQ is trapped inside NM aggregates.[53] Regardless of the reason, the results with the PQ mixtures show that the algae toxicity

does not automatically decrease just because the NM alone efficiently adsorbs the pesticide (as shown by the chemical analysis). When algae are present, they clearly seem to shift the adsorption equilibrium state, which is in accordance with the study by Schwab *et al.*, (2014)[29] who observed desorption of diuron from carbon nanotubes when algae were added to the test system. Algal cells are excreting extracellular polymeric substances (EPS) composed of macromolecular compounds such as polysaccharides, proteins, uronic acids and non-polymeric substances,[54,55] which can bind to NMs.[56,57] Therefore, desorption of pesticides from the NM surface could also be driven by the presence of EPS, which might have a high affinity for the NM.

3.2.1 Impact of nanomaterial shape. One hypothesis of the study is that the elongated NM adsorb larger amounts pesticide of opposite charge per mass than the spherical NMs and hence reduce algal toxicity by a larger amount. The result from the present study strengthens this theory since the elongated NM reduce algal toxicity already at 4 mg L^{-1} by ~20% and completely at 16 mg L^{-1} (Fig. 5D), while for the spherical NM a three times higher concentration (*i.e.*, 50 mg L^{-1}) is needed to achieve the same toxicity reduction. Using the specific surface
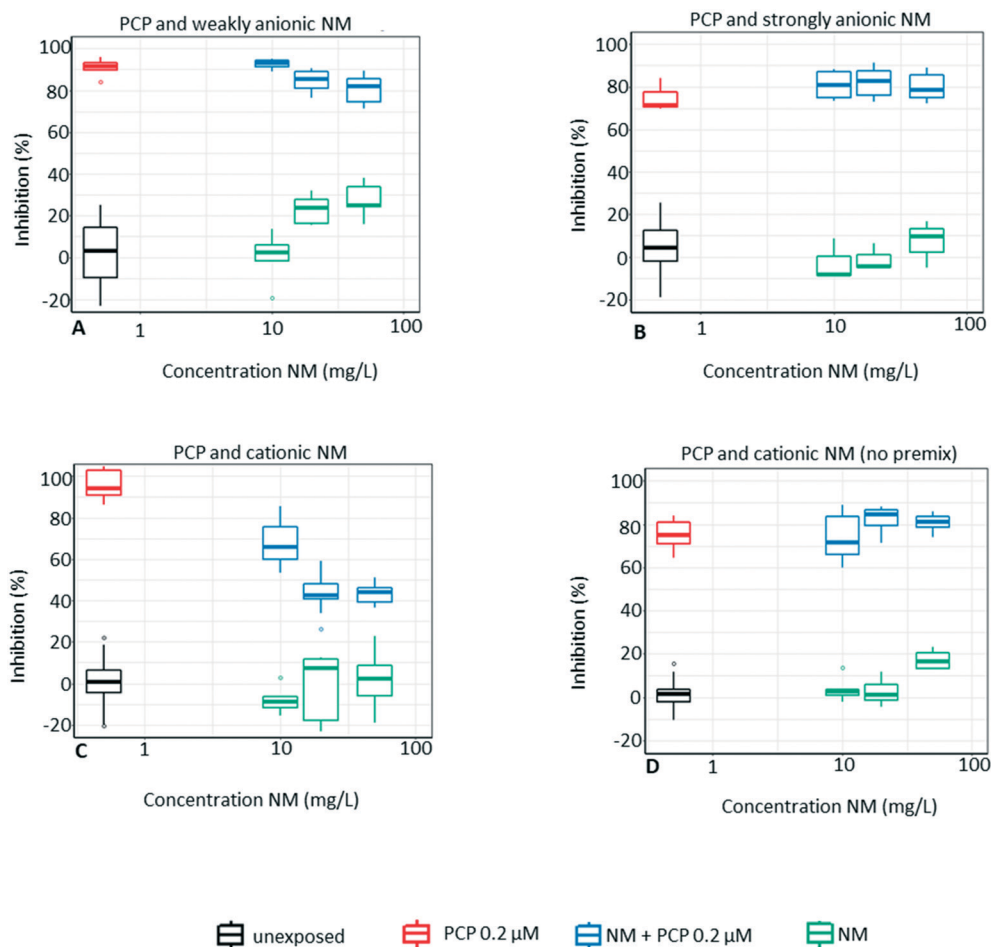
This journal is © The Royal Society of Chemistry 2022

Environ. Sci.: Nano, 2022, **9**, 2402–2416 | **2409**

Fig. 6 Mixture exposures comprising PCP (0.2 μM) and the particles weakly anionic (A), strongly anionic (B), cationic (C) and cationic with no pre-mix (D) at 10, 20 and 50 mg L^{-1} (blue boxes). The black box is the non-treated algae (control), the red box is the inhibition with exposure to only the pesticide and the green box is the inhibition after exposure to only the NM. The boxplots show the median, quartile 1 (Q1), quartile 3 (Q3) and the maximum (Q3 plus 1.5 times the interquartile range) and minimum (Q1 minus 1.5 times the interquartile range).

area as the exposure metric (instead of mass), the difference between spherical and elongated NM is zero (18 m^2 L^{-1} for these two concentrations, see Table 3). The conclusion is therefore

Table 3 Comparison of surface area (SSA) per mass test concentration between the strongly anionic spherical and elongated NMs. The SSAs are calculated from the surface area in the original product, Levasil CS25-436 (360 m^2 g^{-1}) and Levasil RD 2180 (1100 m^2 g^{-1})

Comparison of SSA/mass between the spherical and the elongated NMs

Mass concentration (mg L^{-1})	SSA (m^2 L^{-1}) Levasil CS25–436 (spherical)	SSA (m^2 L^{-1}) Levasil RD 2180 (elongated)
50	18	55
20	7	22
16	6	18
8	3	9
4	1.4	4.4
2	0.7	2.2
1	0.4	1.1
0.4	0.1	0.4

that the surface area and not shape is the factor affecting the adsorption capacity.

3.3 Mixtures with PCP

Cationic NM reduces PCP toxicity by 30% or more at all test concentrations, but only if the mixture of NM and PCP is prepared as a premix 100× the test concentration before it is pipetted into the microtiter plate (Fig. 6C and D). In the premix (1000–5000 mg L^{-1}) the cationic NM have an average size of ~50 nm and a ZP between 30–40 mV. At the actual test concentrations of 10–50 mg L^{-1} the NM agglomerate (average size is now ~1600 nm) and their ZP decrease to around 0 mV, see Table S1.† The cationic charge of the NM in the premix likely facilitates the adsorption of the negatively charged PCP molecules, which might not desorb despite the final 1 : 100 dilution prior to testing. This is also confirmed by the chemical analysis, which shows a 20% reduction in PCP concentration when the test mixture is prepared *via* a 100× concentrated pre-mix, while no reduction occurs if the mixture is prepared directly in the plate (see Table 4).

2410 | *Environ. Sci.: Nano*, 2022, **9**, 2402–2416

This journal is © The Royal Society of Chemistry 2022

Table 4 Pesticide concentration after ultracentrifugation expressed in % of control containing only the pesticide. The values are presented with the average of three replicates and with standard deviation in brackets

Pesticide concentration after ultracentrifugation (%)

Pesticide	Only pesticide	Weakly anionic		Cationic		Strongly anionic		Strongly anionic elongated		
		10 mg L^{-1}	50 mg L^{-1}	10 mg L^{-1}	50 mg L^{-1}	10 mg L^{-1}	50 mg L^{-1}	0.4 mg L^{-1}	16 mg L^{-1}	50 mg L^{-1}
PQ	100 (±5)	82 (±8)	33 (±3)	39 (±10)	10 (±5)	0.5 (±0.1)	0.4 (±0.2)	7 (±3)	0.1 (±0.2)	0.0 (±0.0)
PCP	100 (±0.5)	102 (±1)	107 (±4)	103 (±0.7)	81 (±2)	106 (±1)	106 (±7)			
				101 (±0.8)[a]	100 (±1)[a]					
DFF	100 (±7)	102 (±4)	116 (±2)	95 (±8)	88 (±4)	88 (±7)	84 (±3)			

[a] No pre-mixture.

The pH of the premix is 4.1 for the cationic NM, 8.1 for the strongly anionic NM and 9.0 for the weakly anionic NM. Therefore, only 20% of the PCP molecules in the premix with the cationic NM are actually deprotonated (pK_a 4.7), which is still sufficient for a larger adsorption to the cationic NM, compared to the anionic NM. Interestingly, the calculation of the concentration of deprotonated PCP molecules in the premix (20% based to the pK_a formula), is consistent with the 20% decrease in PCP concentration according to the

chemical analysis, see Table 4. This indicates that the 20% PCP bound to the particles do not desorb when diluted and the pH shifted to neutral, since the pH in all final test concentrations varied within the pH range of 7.2 ± 0.5.

3.4 Mixtures with DFF

The toxicity of DFF is not reduced by co-exposure with weakly or strongly anionic NMs (Fig. 7). However, the algal toxicity is
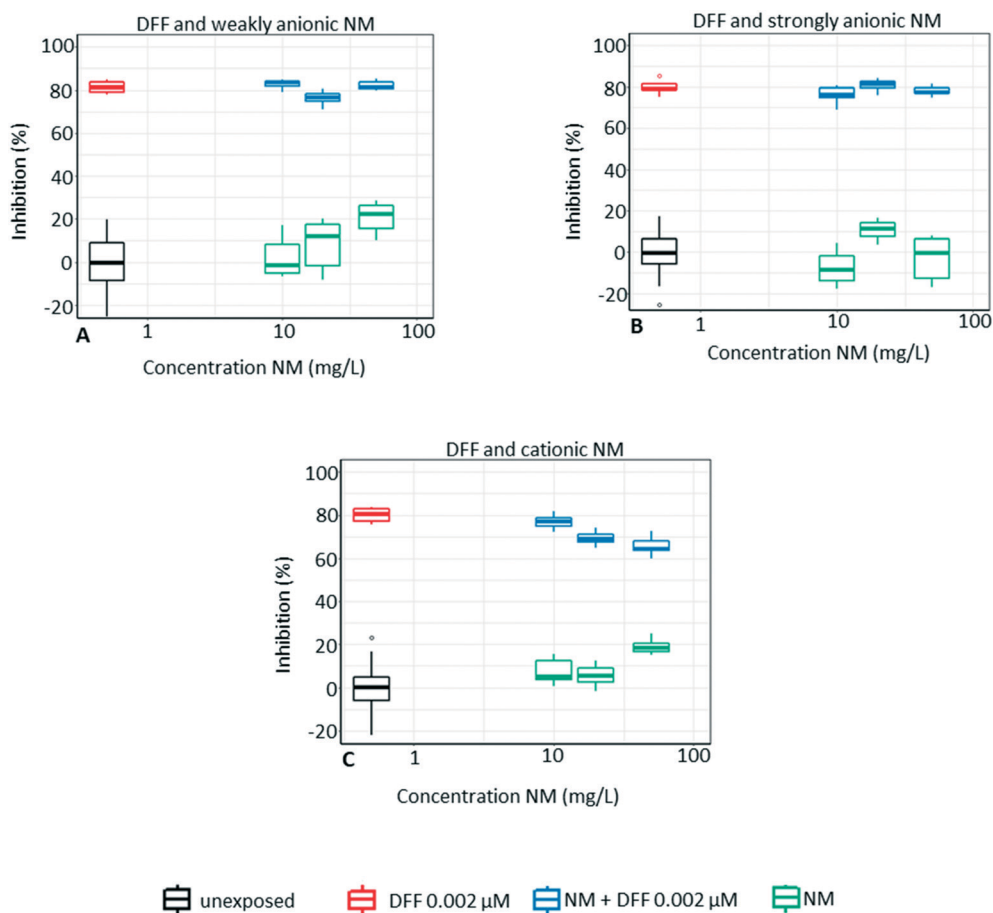

Fig. 7 Mixture exposures comprising of DFF (0.002 μM) and the particles weakly anionic (A), strongly anionic (B), cationic (C) at 10, 20 and 50 mg L^{-1} (blue boxes). The black box is the non-treated algae, *i.e.* the control, the red box is the inhibition with exposure to only the pesticide and the green box is the inhibition after exposure to only particles. The boxplots show the median, quartile 1 (Q1), quartile 3 (Q3) and the maximum (Q3 plus 1.5 times the interquartile range) and minimum (Q1 minus 1.5 times the interquartile range).

This journal is © The Royal Society of Chemistry 2022

Environ. Sci.: Nano, 2022, **9**, 2402–2416 | **2411**

reduced in a concentration-dependant manner by 10–20% in the mixture with the cationic NM and an additional ~20% of the individual toxicity of the cationic NM. This reduction of DFF toxicity is somewhat surprising since we hypothesize that the adsorption would be driven mainly by electrostatic attraction between pesticides and NMs of opposite charges. We speculate that this result could be caused by hydrophobic interaction between the cationic NM, which is almost neutral in algal growth medium (ZP close to 0, -3 ± 3 mV, at t_0, see Table S1†), and the lipophilic DFF ($\log P = 4.2$). The chemical analysis shows a decrease in DFF concentration (~5–10%) for the cationic NM, which supports this hypothesis, see Table 4. However, the chemical analysis also shows a similar reduction in DFF concentration by the strongly anionic NM, which does not reduce algal toxicity. Again, the uptake of DFF by algae could drive desorption of DFF adsorbed onto the strongly anionic NM.

3.5 Silica nanomaterials as adsorbents for charged water pollutants

This paper shows that colloidal silica NMs act as an adsorbent for cationic and anionic charged pollutants and reduce their algal toxicity through retention (reduced toxicity due to a decreased availability of the chemical[31]). Already, 0.4 mg L^{-1} of the elongated NM was able to adsorb 93% of the PQ, which correspond to an adsorption of 957 µg L^{-1}, which is order of magnitudes higher than the allowed limits set for PQ in drinking water, e.g., 0.1 µg L^{-1} by the European Union (COUNCIL DIRECTIVE 98/83/EC of 3 November on the quality of water intended for human consumption, 1998) and 20 µg L^{-1} by the U.S. EPA.[58]

Several experiments investigated the adsorption capacity of PQ onto NMs. Brigante and Schulz[52] report an adsorption capacity of PQ onto titanium functionalized silica nanoparticles of 17 mg g^{-1} particles. Activated carbon adsorbed 6 mg g^{-1},[59] Zeolites 162 mg g^{-1},[60] bentonite modified with mesoporous silica 12 mg g^{-1} (ref. 61) and carbon nanotubes 219 mg g^{-1}.[62] The corresponding adsorption capacity for the elongated silica NM (used in the present study and based on our chemical analysis), would be 2392 mg PQ g^{-1} NM. This seems to be superior to other materials investigated for the adsorption of PQ and similar chemicals in the context of water treatment. The efficient adsorption of the divalent cation PQ observed in the present study suggests that anionic NM could also be suitable materials for other cationic pollutants such as cationic surfactants, heavy metals (which do not adsorb well to activated carbon[63]) and compounds with one or several amine groups.

Adsorption of the anionic model pollutant PCP onto the cationic silica NM seems to be impacted by pH and phosphate concentrations. The MBL medium used here contains a high phosphate concentration (1.5 mg L^{-1}) compared to other growth media or surface waters.[45,64] Further studies are therefore needed to identify the optimal

conditions that facilitate the adsorption of negatively charged contaminants onto cationic functionalized silica NMs. However, the results indicate that acidic conditions and low phosphate content would promote contaminant adsorption.

3.6 Future perspectives and knowledge gaps

Nanotechnology can make an important and sustainable contribution to the production of clean water.[65–69] However, there are several challenges ahead for implementing nano-technological applications, which often revolve around the up-scaling from small laboratory systems to large-scale commercial systems, which requires robust, sustainable, cost-effective approaches that are applicable in situ and or ex situ.[65–69] It is therefore important that the research underpinning such efforts is based on harmonized and standardized approaches that facilitate the comparison and performance evaluation of different NMs.[69]

The current study touches upon several of these aspects. In particular, the tested colloidal silica NMs are commercially available in large quantities and are already used in large-scale applications in the pulp and paper industry. The test chemicals PQ, PCP and DFF represent the characteristics of a broad range of environmentally relevant chemicals and also the test organism, the green algae R. subcapitata is representative for typical primary producers in freshwater systems.

However, several challenges and knowledge gaps remain to be addressed, including evaluation of the adsorption efficiency/capability of colloidal silica in comparison to other NMs, possibilities for recovery and reuse, performance in situ and ex situ, and in industrial water and natural waters. The findings from this study show that the tested silica NMs are not toxic to freshwater algae at concentrations where a significant pesticide adsorption and toxicity reduction can be observed. However, the sensitivity of other organisms than algae (representing different physiologies, morphologies and trophic levels) to colloidal silica in mixture co-existing pollutants needs to be addressed too. Silica NMs (except for alumina-modified strongly anionic) are prone to adsorb onto the algal cell wall, which constitutes a protective barrier, and therefore are unlikely be taken up by the cells.[70] Nanosilica occurs naturally in waters[71–73] and the algal cell wall is a feature to cope with physical stress from particulate matter.[74] Cells of other species/species groups lack a cell wall, therefore NMs (including silica), which can pass plasma membranes, may act as carriers for surface-adsorbed (ionic) pollutants into cells and increase their bioavailability and bio-concentration.[31,75]

4. Conclusions

This study shows that colloidal silica NMs can be efficient adsorbents for oppositely charged pollutants and lower their toxicity toward algal cells. In particular, the strongly anionic NMs seem well suited to adsorb cationic pollutants, such as paraquat which we tested as a model compound. The

cationic NM's capacity to bind weak acids such as pentachlorophenol seems to be affected by factors such as pH and phosphate content as well as the hydrophilicity and the pK_a of the pollutant of interest. These results might open up for the possibility to use colloidal silica in the context of water purifications to remove micro-pollutants.

Conflicts of interest

Frida Book, Eric Carmona, Thomas Backhaus and Tobias Lammel declare no conflicts of interest. Michael Persson was employed as innovation manager at Nouryon and is currently collaborating with Nouryon as a senior advisor while being employed at Chalmers Industriteknik. Nouryon supplied the silica nanomaterials that were tested in the present manuscript but did not otherwise interfere with the study aims & approaches and the interpretation of the study results.

Acknowledgements

References

1 F. D. Guerra, M. F. Attia, D. C. Whitehead and F. Alexis, Nanotechnology for environmental remediation: Materials and applications, *Molecules*, 2018, **23**(7), 1–23, DOI: **10.3390/molecules23071760**.

2 M. Auffan, J. Rose and C. Chaneac, *et al.*, *Nanoethics and Nanotoxicology, Surface Reactivity of Manufactured Nanoparticles*, 2011, DOI: **10.1007/978-3-642-20177-6**.

3 A. Tsuda and N. V. Konduru, The role of natural processes and surface energy of inhaled engineered nanoparticles on aggregation and corona formation, *NanoImpact*, 2016, **2**, 38–44, DOI: **10.1016/j.impact.2016.06.002**.

4 H. Sadegh, G. A. M. Ali and V. K. Gupta, *et al.*, The role of nanomaterials as effective adsorbents and their applications in wastewater treatment, *J. Nanostruct. Chem.*, 2017, **7**(1), 1–14, DOI: **10.1007/s40097-017-0219-4**.

5 C. Hao, G. Xu, Y. Feng, L. Lu, W. Sun and R. Sun, Fluorescence quenching study on the interaction of ferroferric oxide nanoparticles with bovine serum albumin, *Spectrochim. Acta, Part A*, 2017, **184**, 191–197, DOI: **10.1016/j.saa.2017.05.004**.

6 J. O. Otalvaro and M. Brigante, Interaction of pesticides with natural and synthetic solids. Evaluation in dynamic and equilibrium conditions, *Environ. Sci. Pollut. Res.*, 2018, **25**(7), 6707–6719, DOI: **10.1007/s11356-017-1020-0**.

7 Z. Cai, A. D. Dwivedi and W. N. Lee, *et al.*, Application of nanotechnologies for removing pharmaceutically active compounds from water: Development and future trends, *Environ. Sci.: Nano*, 2018, **5**(1), 27–47, DOI: **10.1039/c7en00644f**.

8 A. S. Ganie, S. Bano and N. Khan, *et al.*, Nanoremediation technologies for sustainable remediation of contaminated environments: Recent advances and challenges, *Chemosphere*, 2021, **275**, 130065, DOI: **10.1016/j.chemosphere.2021.130065**.

9 C. Santhosh, V. Velmurugan, G. Jacob, S. K. Jeong, A. N. Grace and A. Bhatnagar, Role of nanomaterials in water treatment applications: A review, *Chem. Eng. J.*, 2016, **306**, 1116–1137, DOI: **10.1016/j.cej.2016.08.053**.

10 L. Cao, Z. Zhou and S. Niu, *et al.*, Positive-Charge Functionalized Mesoporous Silica Nanoparticles as Nanocarriers for Controlled 2,4-Dichlorophenoxy Acetic Acid Sodium Salt Release, *J. Agric. Food Chem.*, 2018, **66**(26), 6594–6603, DOI: **10.1021/acs.jafc.7b01957**.

11 L. Li, Z. Xu, M. Kah, D. Lin and J. Filser, Nanopesticides: A Comprehensive Assessment of Environmental Risk Is Needed before Widespread Agricultural Application, *Environ. Sci. Technol.*, 2019, **53**(14), 7923–7924, DOI: **10.1021/acs.est.9b03146**.

12 M. Liess, L. Liebmann and P. Vormeier, *et al.*, Pesticides are the dominant stressors for vulnerable insects in lowland streams, *Water Res.*, 2021, **201**, 117262, DOI: **10.1016/j.watres.2021.117262**.

13 A. Sharma, A. Shukla and K. Attri, *et al.*, Global trends in pesticides: A looming threat and viable alternatives, *Ecotoxicol. Environ. Saf.*, 2020, **201**(March), 110812, DOI: **10.1016/j.ecoenv.2020.110812**.

14 F. D. Spilsbury, M. S. J. Warne and T. Backhaus, Risk Assessment of Pesticide Mixtures in Australian Rivers Discharging to the Great Barrier Reef, *Environ. Sci. Technol.*, 2020, **54**(22), 14361–14371, DOI: **10.1021/acs.est.0c04066**.

15 Z. Li and P. Fantke, Toward harmonizing global pesticide regulations for surface freshwaters in support of protecting human health, *J. Environ. Manage.*, 2022, **301**(June 2021), 113909, DOI: **10.1016/j.jenvman.2021.113909**.

16 K. S. Rajmohan, R. Chandrasekaran and S. Varjani, A Review on Occurrence of Pesticides in Environment and Current Technologies for Their Remediation and Management, *Indian J. Microbiol.*, 2020, **60**(2), 125–138, DOI: **10.1007/s12088-019-00841-x**.

17 M. Brigante and P. C. Schulz, Adsorption of paraquat on mesoporous silica modified with titania: Effects of pH, ionic strength and temperature, *J. Colloid Interface Sci.*, 2011, **363**(1), 355–361, DOI: **10.1016/j.jcis.2011.07.061**.

18 L. Cao, H. Zhang, C. Cao, J. Zhang, F. Li and Q. Huang, Quaternized chitosan-capped mesoporous silica nanoparticles as nanocarriers for controlled pesticide release, *Nanomaterials*, 2016, **6**(7), 1–13, DOI: **10.3390/nano6070126**.

This journal is © The Royal Society of Chemistry 2022

Environ. Sci.: Nano, 2022, **9**, 2402–2416 | **2413**

19 Y. Zhang, X. Li and H. Yu, Toxicity of nanoparticle surface coating agents: Structure-cytotoxicity relationship, *J. Environ. Sci. Health, Part C: Environ. Carcinog. Ecotoxicol. Rev.*, 2016, **34**(3), 204–215, DOI: **10.1080/10590501.2016.1202762**.

20 F. Lu and D. Astruc, Nanomaterials for removal of toxic elements from water, *Coord. Chem. Rev.*, 2018, **356**, 147–164, DOI: **10.1016/j.ccr.2017.11.003**.

21 A. S. Adeleye, J. R. Conway, K. Garner, Y. Huang, Y. Su and A. A. Keller, Engineered nanomaterials for water treatment and remediation: Costs, benefits, and applicability, *Chem. Eng. J.*, 2016, **286**, 640–662, DOI: **10.1016/j.cej.2015.10.105**.

22 C. Fruijtier-Pölloth, The toxicological mode of action and the safety of synthetic amorphous silica-A nanostructured material, *Toxicology*, 2012, **294**(2–3), 61–79, DOI: **10.1016/j.tox.2012.02.001**.

23 K. Van Hoecke, K. A. C. De Schamphelaere, S. Ramirez-Garcia, P. Van der Meeren, G. Smagghe and C. R. Janssen, Influence of alumina coating on characteristics and effects of SiO2 nanoparticles in algal growth inhibition assays at various pH and organic matter contents, *Environ. Int.*, 2011, **37**(6), 1118–1125, DOI: **10.1016/j.envint.2011.02.009**.

24 F. Book, M. T. Ekvall and M. Persson, *et al.*, Ecotoxicity screening of seven different types of commercial silica nanoparticles using cellular and organismic assays: Importance of surface and size, *NanoImpact*, 2019, **13**(December 2018), 100–111, DOI: **10.1016/j.impact.2019.01.001**.

25 Nouryon, *Levasil Colloidal Silica Functionality*, **https://prod-colloidalsilica.an-basc.com/functions/**, Published 2021, Accessed August 25, 2021.

26 S. Iravani, Nanomaterials and nanotechnology for water treatment: recent advances, *Inorg. Nano-Met. Chem.*, 2020, 1–31, DOI: **10.1080/24701556.2020.1852253**.

27 M. Persson, M. Tokarz, M.-L. Dahlgren and H. Johansson-Vestin, Patent Application Publication, Patent Number, US 2011/0207128A1, 2011, vol. 1(19), pp. 10–13. **https://patents.google.com/patent/US7919535?oq=michael+persson+akzo+nobel+2011**.

28 W. O. Roberts and E. R. Griffin, *US Pat.*, Patent Number: 5118727, 1992, (19), **https://patentimages.storage.googleapis.com/4a/40/6a/08585b92679510/US5118727.pdf**.

29 F. Schwab, L. Camenzuli and K. Knauer, *et al.*, Sorption kinetics and equilibrium of the herbicide diuron to carbon nanotubes or soot in absence and presence of algae, *Environ. Pollut.*, 2014, **192**, 147–153, DOI: **10.1016/j.envpol.2014.05.018**.

30 N. B. Hartmann and A. Baun, The nano cocktail: ecotoxicological effects of engineered nanoparticles in chemical mixtures, *Integr. Environ. Assess. Manage.*, 2010, **6**(2), 311–313.

31 S. Naasz, R. Altenburger and D. Kühnel, Environmental mixtures of nanomaterials and chemicals: The Trojan-horse phenomenon and its relevance for ecotoxicity, *Sci. Total Environ.*, 2018, **635**, 1170–1181, DOI: **10.1016/j.scitotenv.2018.04.180**.

32 I. Martín-de-Lucía, M. C. Campos-Mañas and A. Agüera, *et al.*, Reverse Trojan-horse effect decreased wastewater toxicity in the presence of inorganic nanoparticles, *Environ. Sci.: Nano*, 2017, 1–26, DOI: **10.1039/C6EN00708B**.

33 J. Cui, T. Liu, F. Li, J. Yi, C. Liu and H. Yu, Silica nanoparticles alleviate cadmium toxicity in rice cells: Mechanisms and size effects, *Environ. Pollut.*, 2017, **228**, 363–369, DOI: **10.1016/j.envpol.2017.05.014**.

34 J. Cui, Y. Li, Q. Jin and F. Li, Silica nanoparticles inhibit arsenic uptake into rice suspension cells: Via improving pectin synthesis and the mechanical force of the cell wall, *Environ. Sci.: Nano*, 2020, **7**(1), 162–171, DOI: **10.1039/c9en01035a**.

35 J. Ma, S. Wang, P. Wang, L. Ma, X. Chen and R. Xu, Toxicity assessment of 40 herbicides to the green alga Raphidocelis subcapitata, *Ecotoxicol. Environ. Saf.*, 2006, **63**(3), 456–462, DOI: **10.1016/j.ecoenv.2004.12.001**.

36 J. Rydh Stenström, J. Kreuger and W. Goedkoop, Pesticide mixture toxicity to algae in agricultural streams – Field observations and laboratory studies with in situ samples and reconstituted water, *Ecotoxicol. Environ. Saf.*, 2021, **215**, 112153, DOI: **10.1016/j.ecoenv.2021.112153**.

37 C. Y. Chen and J. H. Lin, Toxicity of chlorophenols to Pseudokirchneriella subcapitata under air-tight test environment, *Chemosphere*, 2006, **62**(4), 503–509, DOI: **10.1016/j.chemosphere.2005.06.060**.

38 V. Mohaupt, J. Völker and R. Altenburger, *et al.*, Pesticides in European Rivers, Lakes and Groundwaters – Data Assessment, *ETC/ICM Technical Report 1/2020: European Topic Centre on Inland, Coastal and Marine Waters*, 2020.

39 D. A. M. Alexandrino, C. M. R. Almeida, A. P. Mucha and M. F. Carvalho, Revisiting pesticide pollution: The case of fluorinated pesticides, *Environ. Pollut.*, 2022, **292**(PA), 118315, DOI: **10.1016/j.envpol.2021.118315**.

40 A. C. J. H. Johnson, P. Greenwood, M. Hagström, Z. Abbas and S. Wall, Aggregation of nanosized colloidal silica in the presence of various alkali cations investigated by the electrospray technique, *Langmuir*, 2008, **24**(22), 12798–12806, DOI: **10.1021/la8026122**.

41 G. W. Sears, Determination of Specific Surface Area of Colloidal Silica by Titration With Sodium Hydroxide, *Anal. Chem.*, 1956, **28**(12), 1981–1983, DOI: **10.1021/ac60120a048**.

42 T. L. Doane, C. Chuang, R. J. Hill and C. Burda, Nanoparticle ζ –Potentials, *Acc. Chem. Res.*, 2012, **45**(3), 317–326.

43 Wikimedia Commons, **https://commons.wikimedia.org/wiki/Main_Page**, Published 2021, Accessed August 25, 2021.

44 AERU, *PPDB: Pesticide Properties DataBase*, **https://sitem.herts.ac.uk/aeru/ppdb**, Published 2021, Accessed August 25, 2021.

45 H. W. Nichols, *Handbook of Phycological Methods*, ed. J. R. Stein, Camb. Univ. Press. (R. R. L. Guillard, personal communication), 1973, pp. 16–17, Available at: **https://www.marine.csiro.au/microalgae/methods/Media%20CMARC%20recipes.htm#MBL**.

46 T. M. Tsao, Y. M. Chen and M. K. Wang, Origin, separation and identification of environmental nanoparticles: A review, *J. Environ. Monit.*, 2011, **13**(5), 1156–1163, DOI: **10.1039/c1em10013k**.

2414 | *Environ. Sci.: Nano*, 2022, **9**, 2402–2416

This journal is © The Royal Society of Chemistry 2022

47 E. Navarro, A. Baun and R. Behra, et al., Environmental behavior and ecotoxicity of engineered nanoparticles to algae, plants, and fungi, Ecotoxicology, 2008, 17(5), 372–386, DOI: 10.1007/s10646-008-0214-0.

48 C. Wei, Y. Zhang, J. Guo, B. Han, X. Yang and J. Yuan, Effects of silica nanoparticles on growth and photosynthetic pigment contents of Scenedesmus obliquus, J. Environ. Sci., 2010, 22(1), 155–160, DOI: 10.1016/S1001-0742(09)60087-5.

49 S. Manzo, S. Buono, G. Rametta, M. Miglietta, S. Schiavo and G. Di Francia, The diverse toxic effect of SiO2 and TiO2 nanoparticles toward the marine microalgae Dunaliella tertiolecta, Environ. Sci. Pollut. Res., 2015, 22(20), 15941–15951, DOI: 10.1007/s11356-015-4790-2.

50 B. Yao, B. Xi, C. Hu, S. Huo, J. Su and H. Liu, A model and experimental study of phosphate uptake kinetics in algae: Considering surface adsorption and P-stress, J. Environ. Sci., 2011, 23(2), 189–198, DOI: 10.1016/S1001-0742(10)60392-0.

51 J. Jin, S. Liu and J. Ren, Phosphorus utilization by phytoplankton in the Yellow Sea during spring bloom: Cell surface adsorption and intracellular accumulation, Mar. Chem., 2021, 231, 103935, DOI: 10.1016/j.marchem.2021.103935.

52 M. Brigante and P. C. Schulz, Adsorption of paraquat on mesoporous silica modified with titania: Effects of pH, ionic strength and temperature, J. Colloid Interface Sci., 2011, 363(1), 355–361, DOI: 10.1016/j.jcis.2011.07.061.

53 Y. Liu, Y. Nie and J. Wang, et al., Mechanisms involved in the impact of engineered nanomaterials on the joint toxicity with environmental pollutants, Ecotoxicol. Environ. Saf., 2018, 162(June), 92–102, DOI: 10.1016/j.ecoenv.2018.06.079.

54 W. Babiak and I. Krzemińska, Extracellular polymeric substances (EPS) as microalgal bioproducts: A review of factors affecting EPS synthesis and application in flocculation processes, Energies, 2021, 14(13), 4007, DOI: 10.3390/en14134007.

55 S. Naveed, C. Li and X. Lu, et al., Microalgal extracellular polymeric substances and their interactions with metal(loid)s: A review, Crit. Rev. Environ. Sci. Technol., 2019, 49(19), 1769–1802, DOI: 10.1080/10643389.2019.1583052.

56 S. Fulaz, S. Vitale, L. Quinn and E. Casey, Nanoparticle–Biofilm Interactions: The Role of the EPS Matrix, Trends Microbiol., 2019, 27(11), 915–926, DOI: 10.1016/j.tim.2019.07.004.

57 D. W. Hiebner, C. Barros, L. Quinn, S. Vitale and E. Casey, Surface functionalization-dependent localization and affinity of SiO2 nanoparticles within the biofilm EPS matrix, Biofilm, 2020, 2, 100029, DOI: 10.1016/j.bioflm.2020.100029.

58 USEPA W., Edition of the Drinking Water Standards and Health Advisories Tables: United States Environmental Protection Agency. Off Water, 2018, (March).

59 N. K. Hamadi, S. Swaminathan and X. D. Chen, Adsorption of Paraquat dichloride from aqueous solution by activated carbon derived from used tires, J. Hazard. Mater., 2004, 112(1–2), 133–141, DOI: 10.1016/j.jhazmat.2004.04.011.

60 W. Insuwan and K. Rangsriwatananon, Removal of paraquat from aqueous solutions onto zeolite LTL, Eng. J., 2017, 21(2), 15–23, DOI: 10.4186/ej.2017.21.2.15.

61 A. Rasaie, M. M. Sabzehmeidani, M. Ghaedi, M. Ghane-Jahromi and A. Sedaratian-Jahromi, Removal of herbicide paraquat from aqueous solutions by bentonite modified with mesoporous silica, Mater. Chem. Phys., 2021, 262, 124296, DOI: 10.1016/j.matchemphys.2021.124296.

62 H. Li, H. Qi, M. Yin, Y. Chen, Q. Deng and S. Wang, Carbon tubes from biomass with prominent adsorption performance for paraquat, Chemosphere, 2021, 262, 127797, DOI: 10.1016/j.chemosphere.2020.127797.

63 M. Sweetman, S. May and N. Mebberson, et al., Activated Carbon, Carbon Nanotubes and Graphene: Materials and Composites for Advanced Water Purification, C, 2017, 3(4), 18, DOI: 10.3390/c3020018.

64 OECD, OECD Guidelines for the testing of Chemicals. Freshwater Alga and Cyanobacteria, Growth Inhibition Test, Organ Econ Coop Dev, 2011, (April), pp. 1–25, DOI: 10.1787/9789264203785-en.

65 M. Anjum, R. Miandad, M. Waqas, F. Gehany and M. A. Barakat, Remediation of wastewater using various nano-materials, Arabian J. Chem., 2019, 12(8), 4897–4919, DOI: 10.1016/j.arabjc.2016.10.004.

66 M. Ghadimi, S. Zangenehtabar and S. Homaeigohar, An Overview of the Water Remediation Potential of Nanomaterials and Their Ecotoxicological Impacts, Water, 2020, 12(4), 1150, DOI: 10.3390/w12041150.

67 R. Kuhn, I. M. Bryant, R. Jensch and J. Böllmann, Applications of Environmental Nanotechnologies in Remediation, Wastewater Treatment, Drinking Water Treatment, and Agriculture, 2022, pp. 54–90.

68 A. G. Leonel, A. A. P. Mansur and H. S. Mansur, Advanced Functional Nanostructures based on Magnetic Iron Oxide Nanomaterials for Water Remediation: A Review, Water Res., 2021, 190, 116693, DOI: 10.1016/j.watres.2020.116693.

69 H. Lu, J. Wang, M. Stoller, T. Wang, Y. Bao and H. Hao, An overview of nanomaterials for industrial wastewater treatment, Korean J. Chem. Eng., 2019, 36(8), 1209–1225, DOI: 10.1007/s11814-019-0306-y.

70 F. Book and T. Backhaus, Aquatic ecotoxicity of manufactured silica nanoparticles: A systematic review and meta-analysis, Sci. Total Environ., 2022, 806, 150893, DOI: 10.1016/j.scitotenv.2021.150893.

71 H. H. Dürr, M. Meybeck, J. Hartmann, G. G. Laruelle and V. Roubeix, Global spatial distribution of natural riverine silica inputs to the coastal zone, Biogeosciences, 2011, 8(3), 597–620, DOI: 10.5194/bg-8-597-2011.

72 D. Cheng, H. Liu, Y. E, F. Liu, H. Lin and X. Liu, Effects of natural colloidal particles derived from a shallow lake on the photodegradation of ofloxacin and ciprofloxacin, Sci. Total Environ., 2021, 773, 145102, DOI: 10.1016/j.scitotenv.2021.145102.

73 Y. Wang, A. Kalinina, T. Sun and B. Nowack, Probabilistic modeling of the flows and environmental risks of nano-silica, Sci. Total Environ., 2016, 545–546, 67–76, DOI: 10.1016/j.scitotenv.2015.12.100.

This journal is © The Royal Society of Chemistry 2022

Environ. Sci.: Nano, 2022, 9, 2402–2416 | 2415

74 A. Holzinger, K. Herburger, F. Kaplan and L. A. Lewis, Desiccation tolerance in the chlorophyte green alga Ulva compressa: does cell wall architecture contribute to ecological success?, *Planta*, 2015, **242**(2), 477–492, DOI: **10.1007/s00425-015-2292-6**.

75 D. S. T. Martinez, L. J. A. Ellis and G. H. Da Silva, *et al.*, Daphnia magna and mixture toxicity with nanomaterials – Current status and perspectives in data-driven risk prediction, *Nano Today*, 2022, **43**, 101430, DOI: **10.1016/j. nantod.2022.101430**.

2416 | *Environ. Sci.: Nano*, 2022, **9**, 2402–2416

This journal is © The Royal Society of Chemistry 2022